JOURNAL OF RADIATION INDUSTRY

Original article

16(1) : 41-52 (2022)
https://doi.org/10.23042/radin.2022.16.1.41

# Identification of *S*-nitrosylated Proteins in *Arabidopsis thaliana* after Gamma Irradiation

Chuloh Cho[1,2,†], Shubhpreet Kaur[1,3,†], Vandan Nagar[1,4], Dong Ho Bak[1], Gaseul Lee[5], Jeong Hee Moon[5], Kwang-Woo Jung[1], Sungbeom Lee[1,3], Byung Yeoup Chung[1] and Seung Sik Lee[1,3,*]

[1]Advanced Radiation Technology Institute, Korea Atomic Energy Research Institute, Jeongeup 56212, Republic of Korea
[2]Crop Foundation Research Division, National Institute of Crop Science, RDA, Wanju 55365, Republic of Korea
[3]Department of Radiation Science, University of Science and Technology, Daejeon 34113, Republic of Korea
[4]Food Technology Division, Bhabha Atomic Research Centre, Mumbai 400085, India
[5]Disease Target Structure Research Center, Korea Research Institute of Bioscience and Biotechnology, Daejeon 34141, Republic of Korea

**Abstract** Nitric oxide (NO), an important gaseous signaling molecule and reactive nitrogen species (RNS), regulates several developmental processes and stress responses in plants via protein *S*-nitrosylation, in which specific cysteine thiols are converted to *S*-nitrosothiols (SNOs). However, there is no information available regarding the formation of nitrosothiols in *Arabidopsis* due to gamma radiation. In this study, *S*-nitrosylated proteins were detected using the biotin switch method and iodoTMT labeling. After gamma irradiation, *S*-nitrosylated proteins increased in a dose-dependent manner. Using iodoTMT labeling, we identified 178 proteins following a site-specific nitrosoproteomic approach due to the 250 Gy dose of gamma irradiation. The identified proteins belonged to different functional families, including photosynthesis (19.9%), metabolism (10.8%), redox processes (10.2%), protein processing (10.2%), protein synthesis (10.2%), miscellaneous (6.3%), and others. Among them, we selected high-scoring proteins, such as AtPrx and AtTDX, and verified their *S*-nitrosylation through two purified proteins by immunoblotting. This study will be beneficial in understanding the biological effects of radiation.

**Key words:** *Arabidopsis*, Gamma radiation, Nitric oxide, Reactive nitrogen species, *S*-nitrosylation

## 1. INTRODUCTION

Nitric oxide (NO) is a gaseous molecule that diffuses readily through membranes and plays various unprecedented roles in living organisms. It was initially known as an air pollutant, and was later identified as an important signaling molecule. In animals, NO plays a role in immune responses, neurotransmission, cardiovascular homeostasis, apoptosis, and cell proliferation [1]. In plants, NO regulates various growth and developmental processes, such as germination, stomatal closure, root growth, and hormone regulation [2-4]. NO and its derivative reactive nitrogen species (RNS) transmit their bioactivity via *S*-nitrosylation, a reversible post-translational modification (PTM) in which the NO moiety covalently binds to the thiol group of cysteine residues to form *S*-nitrosothiols (SNOs). Numerous studies have shown that *S*-nitrosylation of plant proteins regulates various cellular functions and signaling events in response to biotic and abiotic stresses [5,6]. Numerous factors, such as metals, light, and reducing agents, affect the stability of nitrosothiols (SNOs) in biological samples.

Various proteomic methods have been developed for the identification and quantification of nitrosothiols [7].

http://www.ksri.kr/

Copyright © 2022 by
Korean Society of Radiation Industry

[†]These authors contributed equally to this work.
***Corresponding author.** Seung Sik Lee
Tel. +82-63-570-3332 Fax. +82-63-570-3339 E-mail. sslee@kaeri.re.kr
**Received** 16 February 2022 **Revised** 21 March 2022 **Accepted** 29 March 2022

Generally, nitrosylation is induced by NO donors (such as GSNO) to study the SNO-modification sites in proteins. It is very difficult to compare research based on NO donors via *in vivo* studies in which *S*-nitrosylation occurs to a lesser extent. The identification of nitrosylated proteins induced by *in vivo* conditions requires highly sensitive and specific detection methods. The most frequently used methods for detection are based on the biotin switch technique, in which a reversible biotin-HPDP reagent is added to replace *S*-nitrosylated cysteine (SNO-Cys), which can be further indirectly detected and identified by antibodies or mass spectrometry [8]. However, these methods have limited usage due to false-positive identifications, lack of an appropriate control, insufficient replicates in experimental design, or the need for high doses of NO donors [9]. Recently, Qu *et al*. [9] developed a mass spectrometry (MS)-based selective isobaric tag-labeling method in which proteins are attached to different tags (Iodoacetyl Tandem Mass Tag™, iodoTMT™ 126-131). These iodoTMT reagents irreversibly label-free sulfhydryl groups (-SH groups) on cysteine residues and selectively enrich them with immobilized anti-TMT antibody resin and TMT elution buffer. These selectively enriched proteins were then fragmented to produce reporter ions of specific masses to be identified using liquid chromatography-mass spectrometry (LC-MS/MS). Isobaric mass tag-based methods have been successfully used to profile and quantify *S*-nitrosylated proteins in murine BV-2 microglial cells [10], *Escherichia coli* [11], and synaptosomes [12].

When exposed to ionizing radiation, living cells suffer biological and chemical changes as a direct effect and the production of reactive oxygen and nitrosative species through radiolysis of water as an indirect effect, which leads to damage to biomolecules such as proteins, lipids, and nucleic acids, thereby disturbing oxidative metabolism [13]. To understand the effects of gamma radiation and the response mechanisms of plants, a large amount of work has been conducted at the gene, mRNA, and protein levels. However, little research has been conducted to study the effects of gamma radiation on the post-translational modifications of proteins. In animal studies, there have been few reports on the effects of gamma irradiation on post-translational modification levels. Nicoloas *et al*. [14] reported that SNO proteins are differentially modulated depending on the dose of gamma radiation, which in turn affects the major signaling pathways, such as the neuronal oxide synthase signaling pathway. However, the effects of gamma irradiation at the PTM level in plants should be investigated.

In this study, we identified *S*-nitrosylated proteins produced by gamma irradiation in *Arabidopsis thaliana* and categorized them into functional classes of proteins. In addition, we selected two high-scoring proteins and confirmed their *S*-nitrosylation with the two purified proteins by western blotting.

## 2. MATERIALS AND METHODS

### 2.1. Materials

All chemicals for the biotin switch assay were purchased from Sigma-Aldrich (St. Louis, MO, USA) and used without further purification. N-(2-hydroxyethyl) piperazine-N-(2-ethanesulfonic acid) (HEPES) solution, ethylenediaminetetraacetic acid (EDTA), and neocuproine were used for biotin labeling and protein extraction. Sodium dodecyl sulfate (SDS) and methyl methane thiosulfonate (MMTS) were used to effectively block free thiols. The dual-color protein molecular size standards used in PAGE were obtained from Bio-Rad Laboratories (Hercules, CA, USA).

### 2.2. Plant material and gamma irradiation

*A. thaliana* (Columbia-0 ecotype) seeds were surface-sterilized for 7 min in 4% sodium hypochlorite solution and rinsed six times with sterile water. Seeds were sown on half-strength Murashige and Skoog (1/2 MS) medium (pH 5.7) supplemented with 0.05% MES, 1% sucrose, and 0.6% Phyto Agar, and then stratified in the dark at 4°C for 3 d. Plants were grown at 22°C, and 14-day-old seedlings were irradiated with 50, 250, and 500 Gy of gamma radiation at dose rates of 12.5, 62.5, and 125 $Gyh^{-1}$ for 4 h using a $^{60}Co$ gamma-irradiator (IR-222, MDS Nordion Inc., Kanata, Canada) at the Advanced Radiation Technology Institute (ARTI), Korea Atomic Energy Research Institute (KAERI).

### 2.3. Total protein extraction

The *S*-nitrosylation assay was conducted in two independent biological experiments. Frozen *Arabidopsis* seedlings were ground to a fine powder in a mortar with

liquid nitrogen. The proteins were then extracted with a HEN buffer (250 mM HEPES, pH 7.7, 1 mM EDTA, 0.1 mM neocuproine) and protease inhibitor cocktail (Sigma-Aldrich) for biotin labeling, and a HENS buffer for iodoTMT labeling. The total protein content was quantified by the BCA assay (Thermo Fisher Scientific, Rockford, IL, USA).

### 2.4. Biotin labeling of *S*-nitrosylated proteins

*S*-nitrosylated proteins were analyzed using a biotin-switch assay. Briefly, total protein samples from the 0, 50, 250, and 500 Gy irradiated plants were prepared at a concentration of 1 mg $mL^{-1}$ in ice-cold HEN buffer. Approximately 1 mg of the sample was blocked using blocking buffer (250 mM HEPES, pH 7.7, 1 mM EDTA, 0.1 mM neocuproine, 2.5% SDS, 25 mM *S*-methyl methane thiosulfonate) and incubated at 50°C for 1 h with frequent vortexing. The sample was precipitated by adding two volumes of ice-cold acetone and washing three times with 70% acetone. The pellet was dissolved in 500 μL of HENS buffer (HEN buffer supplemented with 1% SDS) before the addition of 50 μL of 1 M sodium ascorbate (freshly prepared) and 10 μL of 20 mM N-[6-(Biotinamido)hexyl]-3-(2-pyridyldithio)-propionamide (biotin-HPDP). After labeling for 90 min at 25°C, the proteins were precipitated with two volumes of ice-cold acetone. The pellet was resuspended in 200 μL of HEN buffer, and the protein concentration was determined and stored at −20°C.

### 2.5. Gel electrophoresis and western-blot analysis

The biotinylated proteins were separated using 12% SDS-PAGE, transferred to a PVDF membrane, and blocked with 2% BSA. Anti-biotin mouse antibody conjugated with horseradish peroxidase was diluted 1 : 10000, and the enhanced chemiluminescence (ECL) select western blotting detection reaction (GE Healthcare, Chicago, IL, USA) was used to detect the proteins.

### 2.6. iodoTMT™ labeling of *S*-nitrosylated proteins

Protein samples from the 0 and 250 Gy irradiated plants were prepared at a concentration of 1 mg $mL^{-1}$ in HENS buffer. These samples were individually labeled with iodoTMT simplex labeling reagent according to the prescribed protocol (Thermo Scientific). Samples were further digested, desalted, enriched, and analyzed by MS. Briefly, protein samples were treated with MMTS (20 mM final concentration) at 25°C for 30 min with frequent vortexing (protected from light) to block free cysteine thiols. Excess MMTS was removed by acetone precipitation at −20°C for 1 h. The pellets were resuspended in 500 μL of HENS buffer and reduced with 20 μL of 1 M sodium ascorbate in water. Each sample was immediately labeled with 10 μL of iodoTMT labeling reagent (0.2 mg in 10 μL of LC/MS grade methanol) at 37°C for 1 h while protected from light. Excess iodoTMT reagent was quenched with 0.5 M dithiothreitol (DTT, 20 mM final concentration) at 37°C for 15 min (protected from light). Excess DTT was removed by acetone precipitation at −20°C for 1 h. The pellets were resuspended in 500 μL of HENS buffer and alkylated with 100 μL of 0.5 M iodoacetamide at 37°C for 1 h. Proteins were precipitated with acetone at −20°C for 1 h to remove excess iodoacetamide, and the pellets were dried.

### 2.7. Enrichment of iodoTMT-labeled peptides

The pellets were resuspended in 100 μL of 1× TBS buffer (150 mM NaCl, 50 mM Tris, pH 8.0). The protein samples were incubated with 200 μL of anti-TMT resin (Sigma-Aldrich) for 2 h at room temperature (25°C) with end-over-end mixing. The supernatant was removed and the resin was washed five times with 1 mL of TBS followed by three washes with 1 mL HPLC-grade water. Peptides were eluted with 500 μL of TMT elution buffer and precipitated with acetone at −20°C overnight. The supernatant was then collected and analyzed by LC-MS/MS.

### 2.8. Analysis of *S*-nitrosylated proteins and peptides by LC-MS/MS

Rapigest (0.2%) was added to the samples to a final concentration of 0.1%. Approximately 0.3 μg of modified trypsin (Promega, p/n V5111) was added to each sample and incubated for 7 h at 37°C. Rapigest was removed by 1% TFA treatment and centrifugation. The solution was desalted using a C18 spin column (Pierce, P/N89870), and the eluted peptides were vacuum-dried.

The peptides were resuspended in a 2% acetonitrile/ and 0.1% formic acid solution and then injected into the LC-MS/MS system. Briefly, peptides were separated and analyzed using an Easy-nanoLC1000 and LTQ-Orbitrap Elite (Thermo Fisher Scientific, Waltham, MA, USA). The trap column was an Acclaim PepMap 100 (75 μm × 2 cm, C18, 3 μm, 100Å) C18 LC column (Thermo Fisher Scientific), and the analytical column was a PepMap RSLC C18 (2 μm, 100Å, 75 μm × 50 cm). The column temperature was set to 40°C. The mobile phases were 0.1% formic acid in water (solvent A) and 0.1% formic acid in acetonitrile (solvent B). The peptides were separated using a linear gradient from 2% B to 40% B within 120 min at a flow rate of 300 nL $min^{-1}$.

The survey scan settings were as follows: resolution = 60000, Max IT = 200 ms, AGC target = 1E6, and mass range, 350-2000 Th. The selected precursor was fragmented by CID and analyzed using an Orbitrap. The other parameters for MS/MS scanning were as follows: Top10 double play, max IT = 100 ms, AGC target = 2.5E4, threshold = 2000, normalized collision energy = 35%, isolation width = 3.0, dynamic exclusion parameter repeat count = 1, repeat duration time = 10 s, exclusion list size = 500, and exclusion duration time = 60 s.

The acquired raw file was processed using Proteome Discoverer ver 2.1 (Thermo Fisher Scientific) to generate a mascot generic file (mgf). Mascot ver 2.5 (Matrix Science Ltd., London, UK) was used for peptide identification with the following search parameters: Database = NCBInr limited to *A. thaliana*, Enzyme = Trypsin, variable modification = oxidation (Met), iodoTMT sixplex (on Cys), Missed cleavage = 1, precursor tolerance = 10 ppm, MS/MS tolerance = 0.6 Da, and number of unique sequences ≥ 2.

### 2.9. Cloning, expression, and purification of recombinant proteins

The complete complementary DNA of *AtTDX* and *AtPrxA* were cloned into pET-28a (Novagen, Gibbstown, NJ), and the resultant plasmids were transformed into *E. coli* strain BL21 (DE3). Overexpression of AtTDX and AtPrxA was induced using 0.1 mM isopropyl-β-D-thiogalactopyranoside (IPTG) upon the bacterial culture $OD_{600}$ reaching 0.5-0.6 for a period of 4 h. The culture was harvested, cells were lysed using sonication (VCX 500 W Ultrasonic Processors; Sonics and Materials, Newtown, CT) and the supernatant was loaded onto a nickel-nitrilotriacetate-agarose (Ni-NTA) column (Peptron, Daejeon, Korea) after centrifugation. His-tagged fusion proteins were purified using a Ni-NTA column (Peptron) and eluted by thrombin in thrombin cutting buffer (20 mM Tris-HCl, pH 8.4, 150 mM NaCl) at 4°C overnight to cleave the N-terminal histidine tag and AtTDX or AtPrxA protein. Purified proteins were dialyzed in 50 mM Tris-HCl (pH 8.0) for biochemical analyses. Protein concentrations were estimated by the Bradford method [15] using bovine serum albumin (BSA) as the standard.

### 2.10. *In vitro S*-nitrosylation of recombinant proteins and detection by western blotting

*S*-nitrosylation of recombinant proteins was conducted using the biotin-switch technique, as described previously [16]. Approximately 50 μg of purified recombinant protein in HEN buffer (250 mM HEPES, pH 7.7, 1 mM EDTA) buffer was treated with 250 μM GSNO or 50 μM GSH at 25°C for 30 min in the dark, and the protein was precipitated by adding three volumes of cold acetone. Excessive GSNO or GSH was removed using Amicon Ultra Diafiltration Columns (Merck, Darmstadt, Germany) equilibrated with 50 mM Tris-Cl buffer (pH 8.0), and 170 μL of HENS buffer (HEN buffer supplemented with 1% SDS). The free thiols were blocked by adding MMTS blocking buffer (250 mM HEPES, pH 7.7, 1 mM EDTA, 0.1 mM neocuproine, 2.5% SDS, and 25 mM *S*-methylmethane thiosulfonate) at 50°C for 30 min with frequent vortexing in the dark. After adding 10 μL of 1 M sodium ascorbate and 20 μL of 4 mM biotin-HPDP, the proteins were labeled for 1 h at 25°C. The biotinylated proteins were separated using 12% SDS-PAGE, transferred to a polyvinylidene difluoride (PVDF) membrane, and blocked with 2% BSA. *S*-nitrosylated proteins were detected with an anti-biotin horseradish peroxidase (HRP)-linked antibody (Cell Signaling Technology, Danvers, MA, USA).

## 3. RESULTS AND DISCUSSION

### 3.1. Detection of *S*-nitrosylated proteins after gamma irradiation

The objective of this study was to identify plant pro-

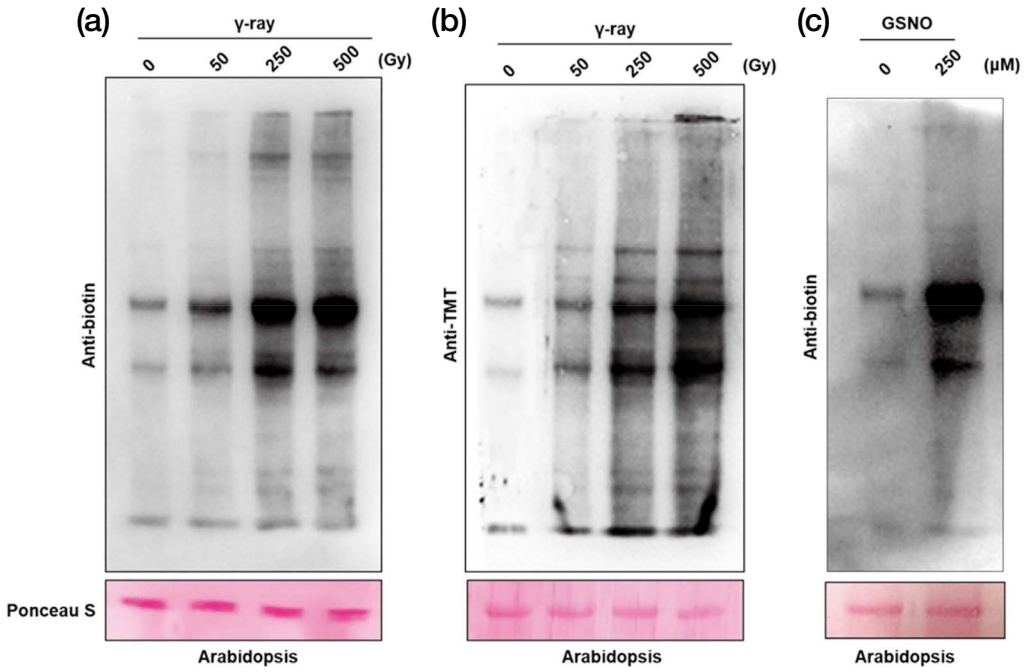


**Fig. 1.** Detection of *S*-nitrosylated proteins in gamma-irradiated *Arabidopsis*. Seedlings were irradiated at different doses (0, 50, 250, and 500 Gy) or treated with 250 μM of GSNO. *S*-nitrosylated proteins were labeled with biotin (a and c) using the biotin switch method and iodoTMT (b). The proteins were separated by SDS-PAGE and detected by western bolt analysis using an anti-biotin (a and c) or anti-TMT (b) antibody, respectively.

teins from *A. thaliana* that are *S*-nitrosylated upon treatment with gamma radiation. Therefore, we checked whether *Arabidopsis* proteins were *S*-nitrosylated after treatment with gamma rays following a variety of methods. Total protein extracts from non-irradiated and irradiated (50, 250, and 500 Gy) two-week-old *Arabidopsis* seedlings were analyzed following a modified biotin switch method. *S*-nitrosylated proteins were labeled with biotin or iodoTMT (Fig. 1) and detected by western blotting using anti-biotin or anti-TMT antibodies. The biotin switch assay is widely used for the detection of the *S*-nitrosylation of proteins, in which NO covalently attaches to their Cys residues. This method consists of three steps: (1) blocking of free thiols by thiol-blocking reagents, such as MMTS, (2) simultaneous reduction of S-NO bonds by ascorbate, and (3) labeling of free thiols with biotin to form biotin-labeled proteins [16]. In this study, we labeled *S*-nitrosylated proteins with biotin and iodoTMT (Fig. 1), and the biotin- or iodoTMT-labeled *S*-nitrosylated proteins were detected by immunoblotting with anti-biotin or anti-TMT antibodies, respectively. After gamma irradiation, biotin- and iodoTMT-labeled protein bands were detected in a dose-dependent manner (Fig. 1). The number of *S*-nitrosylated *Arabidopsis* proteins increased remarkably up to 500 Gy of gamma irradiation. Based on these results, gamma irradiation of 250 Gy was sufficient to induce *S*-nitrosylation. Therefore, a dose of 250 Gy was selected to identify the *S*-nitrosylated proteins by gamma radiation. In addition, we confirmed the presence of *S*-nitrosylated proteins by treatment with 250 μM of *S*-nitrosoglutathione (GSNO), a major NO donor (Fig. 1).

### 3.2. Identification of *S*-nitrosylated proteins in *Arabidopsis* after gamma irradiation

The total plant proteins from non-irradiated and 250 Gy irradiated two-week-old plants were subjected to iodoTMT labeling using iodoTMT simplex$^{TM}$ isobaric label reagent, which contains a sulfhydryl reactive iodoacetyl group that irreversibly labels free sulfhydryl groups on *S*-nitrosylated cysteine residues [10]. The iodoTMT-labeled proteins were selectively isolated by enriching the samples using anti-TMT antibody resin and TMT elution buffer (Fig. 1). Then, the iodoTMT-labeled proteins were digested with trypsin, and the resulting peptides were analyzed using nano-LC/

**Table 1.** *S*-nitrosylated *Arabidopsis* proteins in response to 250 Gy gamma radiation.

| Functional class | Accession | Score | AGI Locus | Description |
|---|---|---|---|---|
| Cell organization | gil15231447 | 78 | At3g46520 | ACT12 (actin-12) |
| | gil1669389 | 31 | At1g49240 | ACT8 (actin 8) |
| | gil3478700 | 21 | At4g35450 | AFT |
| DNA synthesis | gil15226944 | 70 | At2g28740 | HIS4 (histone H4) |
| | gil15224957 | 56 | At2g38810 | HTA8 (histone H2A 8) |
| | gil15232146 | 56 | At3g27360 | H3.1 (histone H3) |
| | gil15227918 | 23 | At2g42320 | Nucleolar protein gar2-like protein |
| | gil15229538 | 23 | At3g23890 | TOPII (DNA topoisomerase 2) |
| Energy | gil15232644 | 63 | At3g15640 | Rubredoxin-like superfamily protein |
| | gil15231176 | 48 | At3g52300 | ATPQ (ATP synthase subunit D) |
| | gil15219886 | 46 | At1g22450 | AtCOX6B2 (cytochrome C oxidase 6B) |
| | gil15226092 | 31 | At2g07698 | ATPase (F1 complex, alpha subunit protein) |
| Metabolism | gil15242465 | 199 | At5g09650 | PPA6 (Pyrophosphorylase 6) |
| | gil30685030 | 145 | At5g14740 | CA2 (Carbonic anhydrase 2) |
| | gil30678347 | 71 | At3g01500 | CA1 (Carbonic anhydrase 1) |
| | gil15224470 | 127 | At2g38230 | PDX1.1 (Pyridoxine biosynthesis 1.1) |
| | gil3746809 | 105 | At5g63400 | ADK1 (Adenylate kinase) |
| | gil16396 | 75 | At4g09320 | NDK1 (Nucleoside diphosphate kinase 1) |
| | gil414550 | 57 | At3g55440 | CTIMC (Cytosolic triose phosphate isomerase) |
| | gil3063661 | 50 | At5g63310 | NDPK1A (Nucleoside diphosphate kinase 1a) |
| | gil18394414 | 48 | At1g16880 | ACR11 (ACT domain-containing protein) |
| | gil15229522 | 45 | At3g23810 | SAHH2 (S-adenosyl-l-homocysteine hydrolase 2) |
| | gil4678346 | 44 | At3g48420 | Haloacid dehalogenase-like hydrolase (HAD) superfamily |
| | gil18415779 | 40 | At4g21860 | MSRB2 (Methionine sulfoxide reductase B2) |
| | gil15231715 | 40 | At3g52930 | FBA8 (Fructose-bisphosphate aldolase) |
| | gil15809938 | 39 | At5g26000 | TGG1 (Thioglucoside glucohydrolase 1) |
| | gil15238559 | 37 | At5g35630 | GSL1 (Glutamine synthetase 2) |
| | gil7769871 | 35 | At1g53240 | MMDH1 (Mitochondrial malate dehydrogenase 1) |
| | gil15229033 | 29 | At3g17390 | MAT4 (Methionine adenosyltransferase 4) |
| | gil15241124 | 26 | At5g28050 | Cytidine/deoxycytidylate deaminase family protein |
| | gil15225353 | 22 | At2g20420 | ATP citrate lyase (ACL) family protein |
| Miscellaneous | gil15234164 | 141 | At4g27520 | ENODL2 (Early nodulin-like protein 2) |
| | gil15233888 | 105 | At4g18480 | LOST1 (Low temperature with open stomata 1) |
| | gil15219200 | 93 | At1g78850 | MBL1 (Mannose binding lectin 1) |
| | gil30696344 | 50 | At5g53490 | TL17 (Thylakoid lumenal 17.4 protein) |
| | gil15239843 | 44 | At5g43330 | C-NAD-MDH2 (Cytosolic-NAD-dependent malate dehydrogenase 2) |
| | gil2827544 | 40 | At4g22670 | HIP1 (HSP interacting protein 1) |
| | gil1272406 | 34 | At3g25220 | FKBP15-1 (FK506-binding protein 15-1) |
| | gil15228869 | 33 | At3g56240 | CCH (Copper chaperone) |
| | gil4455367 | 29 | At4g28080 | TSS (TPR-domain supperssor of STIMPY) |
| | gil973313 | 28 | At2g22420 | MIPS2 (Myo-inositol-1-phosphate synthase 2) |
| | gil30690772 | 26 | At2g47730 | GSTF8 (Glutathione S-transferase phi 8) |
| Photosynthesis | gil15450379 | 368 | At2g39730 | RCA (Rubisco activase) |
| | gil7525041 | 312 | AtCg00490 | RBCL (Rubisco large subunit) |
| | gil22571 | 257 | At5g66570 | PSBO1 (Photosystem II oxygen-evolving complex 1) |
| | gil15233587 | 197 | At4g21280 | PSBQ (Photosystem II subunit Q) |

**Table 1.** Continued.

| Functional class | Accession | Score | AGI Locus | Description |
|---|---|---|---|---|
| Photosynthesis | gil15230595 | 144 | At3g12780 | PGK1 (Phosphoglycerate kinase 1) |
| | gil336390 | 143 | At1g42970 | GAPB (Glyceraldehyde 3-phosphate dehydrogenase B subunit) |
| | gil166702 | 33 | At1g12900 | GAPA (Glyceraldehyde 3-phosphate dehydrogenase A subunit) |
| | gil7525040 | 140 | AtCg00480 | HCF1BET (ATP synthase CF1 beta subunit) |
| | gil15236722 | 117 | At4g32260 | PDE334 (Pigment defective 334) |
| | gil14334740 | 114 | At2g21330 | FBA1 (Fructose-bisphosphate aldolase 1) |
| | gil16226653 | 68 | At4g38970 | FBA2 (Fructose-bisphosphate aldolase 2) |
| | gil7525018 | 107 | AtCg00120 | ATPA (ATP synthase subunit alpha) |
| | gil15233985 | 86 | At4g09650 | ATPD (ATP synthase subunit delta) |
| | gil295792 | 85 | At1g67090 | RBCS1A (Ribulose bisphosphate carboxylase small chain 1A) |
| | gil15240901 | 70 | At5g38410 | RBCS3B (Ribulose bisphosphate carboxylase small chain 3B) |
| | gil15226479 | 80 | At2g21170 | TIM (Triosephosphate isomerase) |
| | gil18379115 | 73 | At1g03600 | PSB27 (Photosystem II family protein) |
| | gil11692884 | 68 | At4g28750 | PSAE-1 (Photosystem I reaction centre subunit IV) |
| | gil15222166 | 67 | At1g06680 | PSBP-1 (Photosystem II subunit P-1) |
| | gil17939849 | 60 | At5g08670 | Mitochondrial F1 ATP synthase beta subunit |
| | gil7525046 | 58 | AtCg00540 | PETA (Photosynthetic electron transfer A) |
| | gil9843639 | 51 | At4g03280 | PETC (Photosynthetic electron transfer C) |
| | gil15234637 | 47 | At4g05180 | PSBQ-2 (Photosystem II subunit Q-2) |
| | gil7329685 | 46 | At3g60750 | TKL1 (Transketolase 1) |
| | gil1143394 | 46 | At4g11150 | VHA-E1 (Vacuolar ATP synthase subunit E1) |
| | gil17473828 | 40 | At1g29910 | CAB3 (Chlorophyll a/b binding protein 3) |
| | gil18407178 | 36 | At2g46820 | PSI-P (Photosystem I P subunit ) |
| | gil15228752 | 32 | At3g62410 | CP12-2 (CP12 domain-containing protein 2) |
| | gil15229497 | 31 | At3g14415 | GOX2 (Aldolase-type TIM barrel family protein) |
| | gil1076373 | 28 | At3g50820 | PSBO2 (Photosystem II  oxygen-evolving complex 2) |
| | gil3892051 | 26 | At4g02580 | NADH-ubiquinone oxidoreducatase 24 kDa subunit |
| | gil11762196 | 24 | At3g15840 | PIFI (Post-illumination chlorophyll fluorescence increase) |
| | gil5730139 | 23 | At5g66190 | FNR1 (Ferredoxin-NADP[ + ]-oxidoreductase 1) |
| | gil5708095 | 20 | At4g04640 | ATPC1 (ATPase, F1 complex, gamma subunit protein) |
| | gil5734518 | 19 | At1g31330 | PSAF (Photosystem I subunit F) |
| Protein processing | gil15226314 | 199 | At2g28000 | CPN60A (Chaperonin 60 alpha) |
| | gil15222729 | 101 | At1g55490 | CPN60B (Chaperonin 60 beta) |
| | gil15230534 | 96 | At3g12580 | HSP70 (Heat shock protein 70) |
| | gil18394184 | 54 | At1g14980 | CPN10 (Chaperonin 10) |
| | gil3057150 | 53 | At5g20720 | CPN20 (Chaperonin 20) |
| | gil15227259 | 53 | At2g16600 | ROC3 (Rotamase CYP 3) |
| | gil11762200 | 53 | At3g62030 | ROC4 (Rotamase CYP 4) |
| | gil18399513 | 51 | At2g20890 | PSB29 (Photosystem II reaction center PSB29 protein) |
| | gil4204267 | 47 | At1g55480 | ZKT (Protein containing PDZ domain, a K-box domain, and a TPR region) |
| | gil1737169 | 45 | At1g75950 | SKP1 (S phase kinase-associated protein 1) |
| | gil18422289 | 44 | At5g43060 | RD21B (Granulin repeat cysteine protease family protein) |
| | gil15242472 | 38 | At5g45680 | FKBP13 (FK506-binding protein 13) |
| | gil15224305 | 34 | At2g43560 | FKBP-like peptidyl-prolyl cis-trans isomerase family protein |
| | gil14423466 | 27 | At2g44650 | CHL-CPN10 (Chloroplast chaperonin 10) |
| | gil15227690 | 21 | At2g03670 | CDC48B (Cell division cycle 48B) |
| | gil6652888 | 18 | At5g19990 | RPT6A (Regulatory particle triple-A ATPase 6A) |
| | gil8778634 | 16 | At1g12490 | F-box associated ubiquitination effector family protein |
| | gil15236211 | 16 | At4g34870 | ROC5 (Rotamase cyclophilin 5) |

**Table 1.** Continued.

| Functional class | Accession | Score | AGI Locus | Description |
|---|---|---|---|---|
| Protein synthesis | gil15232515 | 131 | At3g15190 | PRPS20 (Chloroplast 30S ribosomal protein S20) |
| | gil468773 | 113 | At3g27850 | RPL12-C (Ribosomal protein L12-C) |
| | gil15226231 | 110 | At2g27720 | 60S acidic ribosomal protein family |
| | gil9295717 | 91 | At1g26630 | ELF5A-2 (Eukaryotic elongation factor 5A-2) |
| | gil14517542 | 88 | At1g47128 | RD21A (Responsive to dehydration 21A) |
| | gil30687350 | 85 | At5g19510 | Translation elongation factor EF1B/ribosomal protein S6 family protein |
| | gil15238369 | 78 | At5g65220 | Ribosomal L29 family protein |
| | gil227204273 | 75 | At3g13920 | EIF4A1 (Eukaryotic translation initiation factor 4A1) |
| | gil15237059 | 73 | At4g20360 | RABE1b (RAB GTPase homolog E1B) |
| | gil1279212 | 71 | At4g25130 | MSRA4 (Methionine sulfoxide reductase A4) |
| | gil295789 | 70 | At5g60390 | EF1ALPHA (Elongation factor 1-alpha) |
| | gil18417320 | 59 | At4g29060 | EMB2726 (Embryo defective 2726) |
| | gil15223354 | 55 | At1g32990 | PRPL11 (Plastid ribosomal protein l11) |
| | gil15230476 | 48 | At3g12390 | Nascent polypeptide-associated complex (NAC), alpha subunit family protein |
| | gil15228141 | 37 | At2g04390 | Ribosomal S17 family protein |
| | gil15220742 | 33 | At1g23410 | Ribosomal protein S27a/Ubiquitin family protein |
| | gil15236166 | 32 | At4g34620 | SSR16 (Small subunit ribosomal protein 16) |
| | gil18420800 | 23 | At5g24490 | 30S ribosomal protein |
| Redox | gil21536657 | 1595 | At3g17880 | **AtTDX (Arabidopsis Tetraticopeptide domain-containing thioredoxin)** |
| | gil15229806 | 1185 | At3g11630 | **AtPRXA (Arabidopsis 2-Cys peroxiredoxin A)** |
| | gil18415155 | 1100 | At5g06290 | PRXB (2-Cys peroxiredoxin B) |
| | gil15239136 | 96 | At5g42980 | TRXH3 (Thioredoxin H-type 3) |
| | gil9755723 | 84 | At5g16710 | DHAR3 (Dehydroascorbate reductase 3) |
| | gil15231718 | 78 | At3g52960 | PRXIIE (Peroxiredoxin-II-E) |
| | gil15242674 | 75 | At5g40370 | GRXC2 (Glutaredoxin C2) |
| | gil30678634 | 74 | At1g03680 | TRXM1 (Thioredoxin M-type 1) |
| | gil15230982 | 68 | At3g26060 | PRXQ (Peroxiredoxin Q) |
| | gil6539610 | 58 | At4g03520 | TRXM2 (Thioredoxin M-type 2) |
| | gil15225103 | 56 | At2g31570 | GPX2 (Glutathione peroxidase 2) |
| | gil7658343 | 51 | At3g06050 | PRXIIF (Peroxiredoxin-II-F) |
| | gil15225333 | 49 | At2g20270 | GRXS12 (Chloroplast GRX 12) |
| | gil4973252 | 42 | At3g02730 | TRXF1 (Thioredoxin F-type 1) |
| | gil15223049 | 38 | At1g07890 | APX1 (Ascorbate peroxidase 1) |
| | gil15219086 | 37 | At1g21750 | PDI5 (Protein disulfide isomerase 5) |
| | gil16215 | 36 | At4g35090 | CAT2 (Catalase 2) |
| | gil166706 | 34 | At3g04120 | GAPC1 (Glyceraldehyde 3-phosphate dehydrogenase C subunit) |
| | gil6539614 | 32 | At3g15360 | TRXM4 (Thioredoxin M-type 4) |
| RNA | gil15226605 | 119 | At2g21660 | GRP7 (Glycine-rich RNA-binding protein 7) |
| | gil7671404 | 49 | At3g45030 | RPS20A (Ribsomomal protein S20-1) |
| | gil4539310 | 37 | At4g38910 | BPC5 (Basic pentacysteine 5) |
| | gil475719 | 34 | At4g24770 | RBP31 (31-kDa RNA-binding protein) |
| | gil1255987 | 30 | At2g22840 | GRF1 (Growth-regulating factor 1) |
| | gil6165644 | 24 | At2g28350 | ARF10 (Auxin response factor 10) |
| | gil78484000 | 21 | At1g55870 | PARN (Poly (A) ribonuclease) |
| | gil7523419 | 19 | At3g63370 | PCMP-H83 (Pentatricopeptide repeat-containing protein) |
| | gil15236059 | 15 | At4g31720 | STG1 (Salt tolerance during germination 1) |

**Table 1.** Continued.

| Functional class | Accession | Score | AGI Locus | Description |
|---|---|---|---|---|
| Signaling | gil16223 | 72 | At1g66410 | CAM4 (Calmodulin 4) |
| | gil18395103 | 48 | At1g22300 | GRF10 (General regulatory factor 10) |
| | gil15229836 | 33 | At3g11730 | RABD1 (RAB gtpase homolog D1) |
| | gil15226197 | 30 | At2g01210 | ZAR1 (Zygotic arrest 1) |
| | gil5020168 | 19 | At2g02950 | PKS1 (Phytochrome kinase substrate 1) |
| | gil21593729 | 17 | At4g28390 | AAC3 (ADP/ATP carrier 3) |
| | gil15225805 | 15 | At2g33170 | Leucine-rich repeat receptor-like protein kinase family protein |
| Stress | gil15241102 | 119 | At5g56000 | HSP81.4 (Heat shock protein 81.4) |
| | gil1515105 | 76 | At5g52640 | HSP90.1 (Heat shock protein 90.1) |
| | gil15234010 | 73 | At4g38680 | GRP2 (Glycine rich protein 2) |
| | gil15236566 | 38 | At4g23670 | Polyketide cyclase/dehydrase and lipid transport superfamily protein |
| | gil21536765 | 32 | At1g34000 | OHP2 (One-helix protein 2) |
| | gil158253345 | 32 | At1g10920 | LOV1 (Locus orchestrating victorin effects 1) |
| Unknown | gil15235363 | 147 | At4g20260 | PCAP1 (Plasma-membrane associated cation-binding protein 1) |
| | gil18394322 | 99 | At1g16080 | Nuclear protein |
| | gil12323328 | 71 | | Kinetochore protein NUF2 |
| | gil18399899 | 58 | At2g22170 | PLAT2 (Lipase/lipooxygenase, PLAT/LH2 family protein) |
| | gil2443757 | 45 | | ROC6 (Rotamase cyclophilin 6) |
| | gil9293981 | 40 | At3g20250 | PUM5 (Pumilio 5) |
| | gil18404496 | 30 | At2g37660 | NAD (P)-binding Rossmann-fold superfamily protein |
| | gil334183415 | 29 | At1g58230 | BCHB (Beach-domain homolog B) |
| | gil240254318 | 26 | At1g64790 | ILA (Ilityhia) |
| | gil9759624 | 26 | At5g65440 | Transmembrane protein |
| | gil5732034 | 26 | | Pfam family PF00319, SRF-type transcription factor |
| | gil51971677 | 24 | At1g74900 | OTP43 (Organelle transcript processing defect 43) |
| | gil11994791 | 24 | At3g28830 | Mucin-like protein, putative (DUF1216) |
| | gil18423453 | 24 | At5g52970 | Thylakoid lumen 15.0 kDa protein |
| | gil5882745 | 23 | At1g74790 | Catalytics |
| | gil8778261 | 23 | | Unknown |
| | gil9294588 | 22 | | Ser-Thr protein kinase-like protein |
| | gil9759492 | 22 | | Nuclear pore protein-like |
| | gil15225507 | 19 | At2g45540 | WD-40 repeat family protein/beige-like protein |
| | gil3292830 | 19 | At4g23040 | PUX13 (Plant UBX domain-containing protein 13) |
| | gil11994666 | 18 | | Phosphatidylinositol/phosphatidylcholine transfer protein-like |
| | gil21592509 | 17 | | Unknown |
| | gil6691191 | 16 | | Putative retrotransposon polyprotein |
| | gil1732515 | 15 | | Myosin heavy chain-like protein |

MS/MS. Finally, we identified 178 proteins after gamma irradiation at 250 Gy.

To functionally categorize the proteins, a MapManBIN search (http://ppdb.tc.cornell.edu/dbsearch/searchacc.asp) was conducted using 178 accessions of *A. thaliana*. The 178 *S*-nitrosylated proteins were clustered into 13 functional categories according to MapManBIN (Table 1 and Fig. 2), including photosynthesis (19.9%), metabolism (10.8%), redox processes (10.2%), protein processing (10.2%), protein synthesis (10.2%), miscellaneous (6.3%), RNA processing (4.5%), signaling (4%), stress (3.4%), DNA synthesis (2.8%), energy (2.3%), cell organization (1.7%), and unknown (13.6%) (Fig. 2). 'Photosynthesis' represented the main group (19.9% of

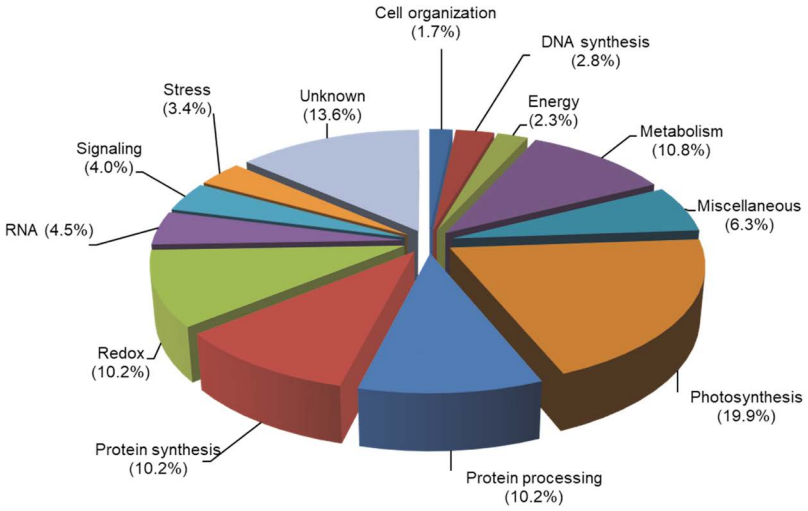


**Fig. 2.** Functional distribution of the 178 identified *S*-nitrosylated proteins exhibiting *S*-nitrosylation due to the 250-Gy gamma radiation dose according to MapManBINs (https://ppdb.tc.cornell.edu/dbsearch/searchacc.aspx).

the total number of proteins), containing enzymes of the components of photosystems I and II, the ATPase complex, Calvin-Benson-Bassham cycle, Rubisco shunt, and photorespiration pathway. The second-most frequent group (10.8%) was involved in metabolism, and the third-most frequent group (10.2%) was involved in redox, protein processing, and synthesis. In total, 13.6% of the proteins could not be functionally annotated or were unknown.

Among the *S*-nitrosylated proteins in *Arabidopsis* after gamma irradiation, the top three proteins (*A. thaliana* tetratricopeptide domain-containing thioredoxin, AtTDX, and 2-Cys peroxiredoxins (AtPrx A, and AtPrx B)) were involved in the redox process (Table 1, highlighted in bold). AtTDX is a thermostable, plant-specific thioredoxin (Trx)-like protein with multiple functions, such as a disulfide reductase and a molecular chaperone, depending on its oligomeric status [17]. 2-Cys Prx contains two conserved Cys residues that function as a peroxidase, molecular chaperone, and protein binding partner. The multiple functions of 2-Cys Prx are associated with its redox-dependent conformation [18]. The protein expression of AtPrx A (At3g11630) and AtPrx B (At5g06290) was induced by gamma irradiation [19]. Additionally, protein expression of the well-known *S*-nitrosylated antioxidant protein ascorbate peroxidase (APX) was induced by gamma irradiation [19]. The multiple functions of AtAPX1 are regulated by posttranslational modifications. *S*-nitrosylation and S-sulfhydration positively modulated peroxidase activity, while it was negatively regulated by tyrosine nitration [20]. Generally, *S*-nitrosylation regulates protein function either positively or negatively, and involves structural changes in proteins. After gamma irradiation, the proteins involved in the redox process were detected as the third-most frequent group (10.2%) containing peroxiredoxin, thioredoxin, glutaredoxin, glutathione peroxidase, ascorbate peroxidase, and catalase, and high scores in *S*-nitrosylated proteins, such as AtTDX, AtPrx A, and AtPrx B, suggesting that not only protein expression, but also functional/or structural regulation of proteins by posttranslational modifications, will play an important role in redox regulation and homeostasis maintenance.

### 3.3. Confirmation of *S*-nitrosylation of AtTDX and AtPrx A

To test whether AtTDX and AtPrx A proteins are *S*-nitrosylated *in vitro*, recombinant AtTDX and AtPrx A proteins were treated with 250 μM of GSNO and subjected to a biotin-switch assay. Free cysteine residues of the GSNO-treated proteins were blocked using thiol-reacting reagent MMTS (alkylation process), and *S*-nitrosylated cysteine (-SNO) residues were then reduced by ascorbate (Asc) for biotin labeling. The biotinylated proteins were detected by western blotting

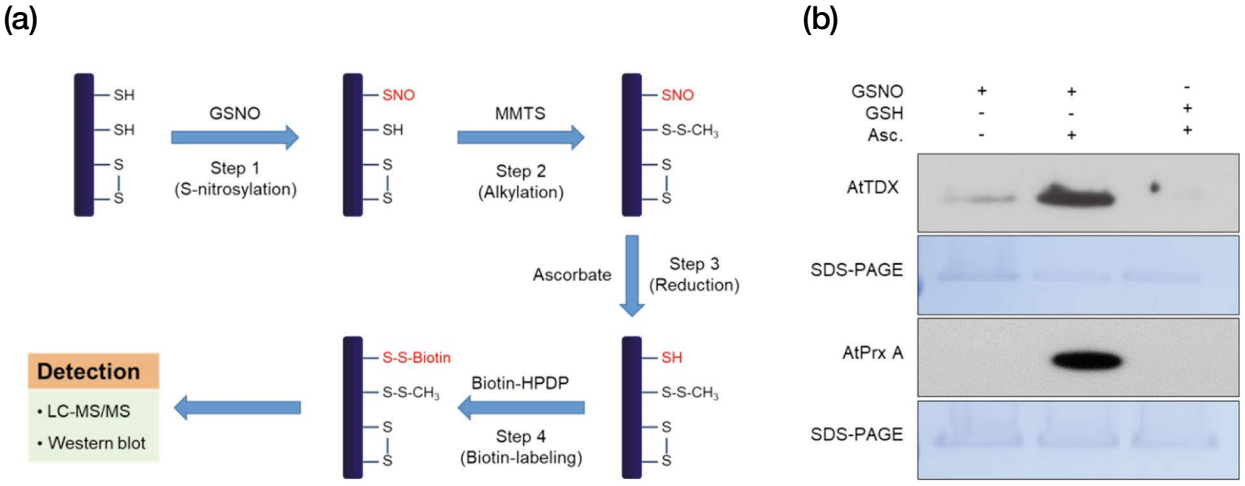


**Fig. 3.** Detection of *S*-nitrosylation of AtTDX and AtPrx A proteins using the modified biotin switch assay. (a) Schematic diagram of the biotin switch assay for detecting *S*-nitrosylation with the following steps: Step 1 (*S*-nitrosylation) - generation of *S*-nitrosylation of proteins, Step 2 (alkylation) - blocking of the free thiols with MMTS, Step 3 (Reduction) - selective reduction of nitrosothiol bonds with ascorbate (Asc), and Step 4 (Biotin-labeling) - labeling of the thiols from formerly *S*-nitrosylated cysteines with the thiol-specific biotinylation reagent biotin-HPDP. Purified recombinant AtTDX and AtPrx A proteins were treated with 250 μM of GSNO (lane 2) or 50 μM of GSH (lane 3), followed by alkylation, reduction, and biotinylation via a slightly modified biotin switch assay as described in the Materials and Methods. The *S*-nitrosylated proteins were separated by SDS-PAGE and detected by western blotting.

using an anti-biotin antibody (Fig. 3a). *S*-nitrosylation of AtTDX and AtPrx A recombinant proteins was highly induced by GSNO and strongly detected by the biotin switch assay (Fig. 3b, lane 2). *S*-nitrosylation (-SNO) is a reversible post-translational modification that is reduced by reducing compounds, such as reduced glutathione (GSH). The proteins treated with 1 mM of GSH without GSNO treatment in lane 3 were reduced to the -SH form, and all free -SH residues were blocked by alkylation with MMTS. Therefore, it was used as a negative control that could not enter the *S*-nitrosylated form (-SNO) (Fig. 3b, lane 3). The results indicated that high scores for two *S*-nitrosylated proteins, AtTDX and AtPrx A, by nano-LC/MS/MS were efficiently verified through the experiment.

## 4. CONCLUSION

In this study, we identified *S*-nitrosylated proteins in *A. thaliana* in response to 250 Gy of gamma radiation following a proteomic approach. *S*-nitrosylation could be effectively detected by the biotin switch method and iodoTMT labeling, and increased in a dose-dependent manner. We identified 178 proteins clustered in 13 functional categories, among which proteins that are involved in redox, such as AtTDX and AtPrx that, were detected with high scores. In addition, *S*-nitrosylation of these proteins was confirmed by western blotting. *S*-ntrosylation is involved in regulation of various cellular functions and signaling events by alterations in protein stability, structure, and function. This finding, which identified *S*-nitrosylation of proteins by gamma irradiation in plants, will provide a lof of information to understand the biological response of radiation.

## ACKNOWLEDGEMENTS

This project was supported by the Nuclear R&D Program of the Ministry of Science and ICT (MSIT), Republic of Korea.

## REFERENCES

1. Zhou L and Zhu D-Y. 2009. Neuronal nitric oxide synthase: Structure, subcellular localization, regulation, and clinical implications. *Nitric Oxide*. **20**:223-230. https://doi.org/10.1016/j.niox.2009.03.001
2. Wilson ID, Ribeiro DM, Bright J, Confraria A, Harrison

J, Barros RS, Desikan R, Neill SJ and Hancock JT. 2009. Role of nitric oxide in regulating stomatal apertures. *Plant Signal. Behav.* **4**:467-469. https://doi.org/10.4161/psb.4.5.8545

3. Freschi L. 2013. Nitric oxide and phytohormone interactions: current status and perspectives. *Front. Plant Sci.* **4**:398. https://doi.org/10.3389/fpls.2013.00398
4. Sun C, Liu L, Zhou W, Lu L, Jin C and Lin X. 2017. Aluminum induces distinct changes in the metabolism of reactive oxygen and nitrogen species in the roots of two wheat genotypes with different aluminum resistance. *J. Agric. Food Chem.* **65**:9419-9427. https://doi.org/10.1021/acs.jafc.7b03386
5. Romero-Puertas MC, Rodríguez-Serrano M, Sandalio LM. 2013. Protein *S*-nitrosylation in plants under abiotic stress: an overview. *Front. Plant Sci.* **4**:373. https://doi.org/10.3389/fpls.2013.00373
6. Zaffagnini M, De Mia M, Morisse S, Di Giacinto N, Marchand CH, Maes A, Lemaire SD and Trost P. 2016. Protein *S*-nitrosylation in photosynthetic organisms: A comprehensive overview with future perspectives. *Biochim. Biophys. Acta.* **1864**:952-966. https://doi.org/10.1016/j.bbapap.2016.02.006
7. Lamotte O, Bertoldo JB, Besson-Bard A, Rosnoblet C, Aimé S, Hichami S, Terenzi H and Wendehenne D. 2014. Protein *S*-nitrosylation: specificity and identification strategies in plants. *Front. Chem.* **2**:114. https://doi.org/10.3389/fchem.2014.00114
8. Jaffrey SR and Snyder SH. 2001. The biotin switch method for the detection of *S*-nitrosylated proteins. *Sci. STKE.* **2001**:pl1. https://doi.org/10.1126/stke.2001.86.pl1
9. Qu Z, Greenlief CM and Gu Z. 2016. Quantitative proteomic approaches for analysis of protein *S*-nitrosylation. *J. Proteome Res.* **15**:1-14. https://doi.org/10.1021/acs.jproteome.5b00857
10. Qu Z, Meng F, Zhou H, Li J, Wang Q, Wei F, Cheng J, Greenlief CM, Lubahn DB, Sun GY, Liu S and Gu Z. 2014. NitroDIGE analysis reveals inhibition of protein *S*-nitrosylation by epigallocatechin gallates in lipopolysaccharide-stimulated microglial cells. *J. Neuroinflammation.* **11**:17. https://doi.org/10.1186/1742-2094-11-17
11. Wojdyla K, Williamson J, Roepstorff P and Rogowska-Wrzesinska A. 2015. The SNO/SOH TMT strategy for combinatorial analysis of reversible cysteine oxidations. *J. Proteomics.* **113**:415-434. https://doi.org/10.1016/j.jprot.2014.10.015
12. Wijasa TS, Sylvester M, Brocke-Ahmadinejad N, Kummer MP, Brosseron F, Gieselmann V and Heneka MT. 2017. Proteome profiling of *S*-nitrosylated synaptosomal proteins by isobaric mass tags. *J. Neurosci. Methods.* **291**:95-100. https://doi.org/10.1016/j.jneumeth.2017.08.005
13. Azzam EI, Jay-Gerin J-P and Pain D. 2012. Ionizing radiation-induced metabolic oxidative stress and prolonged cell injury. *Cancer Lett.* **327**:48-60. https://doi.org/10.1016/j.canlet.2011.12.012
14. Nicolas F, Wu C, Bukhari S, de Toledo SM, Li H, Shibata M and Azzam EI. 2015. *S*-nitrosylation in organs of mice exposed to low or high doses of γ-rays: the modulating effect of iodine contrast agent at a low radiation dose. *Proteomes.* **28**:56-73. https://doi.org/10.3390/proteomes3020056
15. Bradford MM. 1976. A rapid and sensitive method for the quantitation of microgram quantities of protein utilizing the principle of protein-dye binding. *Anal. Biochem.* **72**:248-254. https://doi.org/10.1016/0003-2697(76)90527-3
16. Jaffrey SR, Erdjument-Bromage H, Ferris CD, Tempst P and Snyder SH. 2001. Protein *S*-nitrosylation: a physiological signal for neuronal nitric oxide. *Nat. Cell Biol.* **3**:193-197. https://doi.org/10.1038/35055104
17. Lee JR, Lee SS, Jang HH, Lee YM, Park JH, Park S-C, Moon JC, Park SK, Kim SY, Lee SY, Chae HB, Jung YJ, Kim WY, Shin MR, Cheong G-W, Kim MG, Kang KR, Lee KO, Yun D-J and Lee SY. 2009. Heat-shock dependent oligomeric status alters the function of a plant-specific thioredoxin-like protein, AtTDX. *Proc. Natl. Acad. Sci. U.S.A.* **106**:5978-5983. https://doi.org/10.1073/pnas.0811231106
18. Muthuramalingam M, Seidel T, Laxa M, de Miranda SMN, Gärtner F, Ströher E, Kandlbinder A and Dietz K-J. 2009. Multiple redox and non-redox interactions define 2-cys peroxiredoxin as a regulatory hub in the chloroplast. *Mol. Plant.* **2**:1273-1288. https://doi.org/10.1093/mp/ssp089
19. Jung K-W, Lee D-G, Cho C, Lee S, Kim J-H, Bai H-W, Park Y-D, Chung BY and Lee SS. 2019. Identification of γ-radiation-responsive proteins in *Arabidopsis thaliana*. *J. Radiat. Ind.* **13**:83-91. https://doi.org/10.23042/radin.2019.13.2.83
20. Kaur S, Prakash P, Bak D-H, Hong SS, Cho C, Chung M-S, Kim J-H, Lee S, Bai B-W, Lee SY, Chung BY and Lee SS. 2021. Regulation of dual activity of ascorbate peroxidase 1 from *Arabidopsis thaliana* by conformational changes and posttranslational modifications. *Front. Plant Sci.* **12**:678111. https://doi.org/10.3389/fpls.2021.678111